Nitrogen-containing point defects in multi-crystalline Si solar-cell materials

Haoxiang Zhang,[1] Michael Stavola,[1,a)] and Mike Seacrist[2]
[1]Department of Physics, Lehigh University, Bethlehem, Pennsylvania 18015, USA
[2]MEMC Electronic Materials, St. Peters, Missouri 63376, USA

(Received 3 April 2013; accepted 21 August 2013; published online 5 September 2013)

The multi-crystalline Si used to fabricate solar cells contains nitrogen, with a concentration typically in the mid-10^{15} cm^{-3} range that was introduced by the Si_3N_4 liner of the crucible used for ingot growth. Low temperature infrared spectroscopy has been used to identify and determine the concentrations of the nitrogen-containing point defects in multi-crystalline samples with a range of nitrogen and oxygen concentrations. We find that the dominant nitrogen centers in multicrystalline Si are the NN and NNO_n complexes that are well-known from studies of monocrystalline Si. In as-grown, multi-crystalline Si with an oxygen content of $[O] = 3.2 \times 10^{17}$ cm^{-3}, 44% of the nitrogen was found to be present as NN-O_n complexes. We also found that near 1×10^{14} cm^{-3} NO_n shallow donors can be present. The concentrations of nitrogen centers that also contain oxygen depend strongly on the concentration of oxygen in the multi-crystalline Si substrate. © *2013 AIP Publishing LLC*. [http://dx.doi.org/10.1063/1.4820516]

I. INTRODUCTION

Nitrogen has a low solid-solubility in silicon, near 5×10^{15} cm^{-3} at the melting temperature.[1] Nonetheless, nitrogen impurities play an important role in Si, hardening the material by impeding the motion of dislocations,[2–4] affecting the populations of native vacancies and interstitials produced during crystal growth,[5–9] and interacting with oxygen impurities to form shallow donors.[10–14] Because of nitrogen's effect on the Si materials used for microelectronics applications, its properties have been studied extensively.

The multi-crystalline silicon (mc-Si) that is widely used by industry for the fabrication of solar cells[15,16] contains a substantial concentration of nitrogen impurities that are introduced by the Si_3N_4 liner of the crucible used to contain the Si melt. While Si_3N_4 precipitates can be seen in the mc-Si ingots;[17] only a few studies have investigated the nitrogen point defects that might be present. This paper reports a study of nitrogen-containing point defects in mc-Si produced by directional solidification. Our goal is to apply what is known about nitrogen centers in monocrystalline Si to identify the nitrogen- and oxygen-containing point defects in mc-Si and to determine their concentrations.

A survey of the properties of nitrogen in monocrystalline Si has been presented by Alt and Wagner.[14] The dominant nitrogen center in Si gives rise to a pair of vibrational lines at 764 and 963 cm^{-1} (room temperature) and consists of a pair of N atoms.[18,19] The 963 cm^{-1} line is shown in Fig. 1(a). The structure of the nitrogen pair center was determined by the combination of channeling, infrared (IR) spectroscopy, and theory to consist of a pair of nitrogen split interstitials with antiparallel alignment.[20] The N_iN_i center has the square ring-like structure that is shown in Fig. 1(b) where, in this case, both of the light impurities in the square ring are N atoms.[20,21]

Itoh *et al.* characterized nitrogen-doped Si samples grown by the floating-zone (FZ) method by neutron activation analysis and IR absorption to obtain a calibration of the peak absorption coefficient of the 963 cm^{-1} line (room temperature).[22] The concentration of nitrogen present in the form of NN centers is given by

$$[N] = 1.83 \times 10^{17}\ cm^{-2}\ \alpha_{963}. \quad (1)$$

Not all the nitrogen present was found to be in the form of NN centers in oxygen-rich, Czochralski (Cz)-grown Si.[22] The NN defect can interact with O impurities to form NNO_n centers.[23,24] An example of a NNO_n structure is shown in Fig. 1(b) where the bond-bridging atom shown by a dashed circle is oxygen.[25–27] Additional structures have also been suggested.

In addition to the NN-based structures, a smaller concentration of NO_n structures with a single N atom can form, that are electrically active, shallow donors with a binding energy near 35 meV. These NO_n centers can be studied with high sensitivity by way of their electronic absorption spectra seen in the far-IR.[10,11,13] Studies of the formation of NO_n centers in Si samples with different nitrogen contents established that the NO_n centers contain a single N atom.[12] Theory predicts that the NO center also has a ring-like structure.[25,28] In this case, in the model shown in Fig. 1(b), one of the light impurities in the ring is N and the second is O. This NO structure can include additional O atoms bonded nearby[25,28] [as shown by the dashed circle in Fig. 1(b), as an example] to form a family of up to 8 different shallow donor centers.[14,29,30]

Annealing nitrogen- and oxygen-containing Si at temperatures near 600 °C causes NNO_n and NO_n centers to form at the expense of their bare NN and NO parents.[14,24] Heat treatments at temperatures above 800 °C cause the additional oxygen atoms to be annealed away.

Alt and coworkers have performed a series of detailed experimental studies of the NNO_n and NO_n centers in Czochralski-grown Si.[13,14,29,30] These studies have determined how the various shallow donor centers depend on the

a)Electronic mail: mjsa@Lehigh.edu

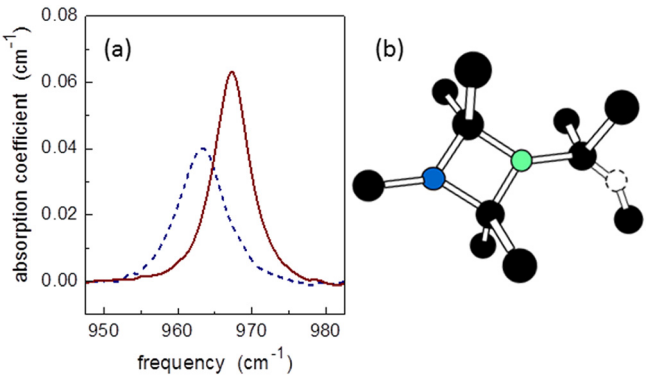

FIG. 1. (a) Absorbance spectra for a mc-Si sample prepared from test slab K(B) (5 mm thickness) annealed at 1000 °C (30 min). The spectrum measured at room temperature is shown by a dashed line; the spectrum measured at 77 K is shown by a solid line. (b) The square ring-like structure of the NN defect, consisting of two antiparallel nitrogen split interstitials. The NO center has a similar structure, where one of the light-element impurities in the ring is N and the second is O. Both the NN and NO defects can bind additional O atoms. The dashed circle shows an additional O atom as an example of such a structure.

N and O content of the Si host[29,30] and on annealing treatments,[14] helping to suggest assignments of the various nitrogen- and oxygen-containing defect centers. The local vibrational modes (LVM's) of NNO_n and NO_n centers seen in the mid-IR have also been investigated.[14]

Kusunoki *et al*. have used IR spectroscopy to show that mc-Si contains NN and NNO_n point defects, similar to the case of Czochralski-grown Si.[31] Their measurements showed that the NN defect concentration was highest at the top of an ingot and that the concentration of NNO_n complexes was higher in the lower part of an ingot. They inferred that NNO_n complexes were formed by the reaction of NN with O during crystal growth.

In the present paper, vibrational spectroscopy is used to determine the concentrations and microscopic identities of NN and NNO_n centers in mc-Si. Far IR measurements are used to identify and determine the concentrations of electrically active NO_n shallow donors.

II. EXPERIMENT

The multi-crystalline Si ingots studied in our experiments were grown in a commercial directional solidification furnace with a charge size of approximately 270 kg in a Si_3N_4-lined crucible. A 4 × 4 matrix of bricks was cut from each ingot. Six test slabs, 156 × 156 mm^2 in size and 2 mm in thickness, and with grains from a few millimeters to a centimeter in size, were cut from the tops and bottoms of three different bricks. Bricks A and E were edge bricks cut from ingots grown at MEMC, and brick K was an interior brick cut from an ingot grown by an external company. The nitrogen concentration of each mc-Si test slab was measured by secondary ion mass spectrometry (SIMS) at QSpec Technology. A few nitrogen-doped, Cz-grown, Si samples were also studied to obtain results that could be contrasted with those for mc-Si.

IR spectra were measured with a Bomem DA3 Fourier transform IR spectrometer. A Si bolometer (4.2 K) with two different cold filters was used to measure spectra in the mid-IR (450–1200 cm^{-1}) and far-IR (200–350 cm^{-1}) ranges. A KBr beamsplitter was used for the mid-IR range and a 3 μm Mylar beamsplitter was used for the far-IR range. Samples were cooled with a Helitran, continuous-flow cryostat to either 77 K for mid-IR measurements or 4.2 K for far-IR measurements.

To characterize the concentrations of carbon and oxygen, the peak absorption coefficients of the IR lines at 607 and 1106 cm^{-1}, respectively, were measured at room temperature for each of the 2 mm thick test slabs. The concentration of substitutional carbon is related to the peak absorption coefficient at 607 cm^{-1} by the relationship[32] $[C] = 1.0 \times 10^{17}\,cm^{-2}\,\alpha_{607}$. The concentration of interstitial oxygen is related to the peak absorption coefficient at 1106 cm^{-1} by the relationship[33] $[O] = 3.15 \times 10^{17}\,cm^{-2}\,\alpha_{1106}$. The concentrations of C and O determined by IR spectroscopy along with the concentrations of nitrogen determined by SIMS for our mc-Si test slabs are listed in Table I. Test slabs labeled by a B designation in parentheses were cut from approximately 34 mm from the bottom of a brick, and samples labeled with a T designation were cut from 34 mm from the top of a brick. The results in Table I show that the O concentration was higher at the bottoms of the mc-Si bricks we investigated, as expected for a Si ingot solidified from the bottom up, consistent with the findings of others.[16,17,31] We cut 3 samples from test slab A(B), spaced apart by 5 cm, to probe the uniformity of the light-impurity concentrations in a test slab. We found the variation in the impurity content for samples prepared from different places in the test slab to be less than 10%.

The vibrational lines for the low concentrations of the nitrogen-containing centers that are of interest here are weak. We cut samples with dimensions 2 × 8 × 5.0 mm^3 from each of the six test slabs so that IR measurements in the mid-IR could be made with a 5 mm optical path length to detect the LVM's of NN-related centers. The intensities of the NN and NNO_n centers were measured at 77 K where their IR lines become narrower than at room temperature and can be detected with greater sensitivity. Unfortunately, it was not possible to make spatially resolved measurements of the NN and NNO_n centers to probe whether nitrogen is preferentially clustered near structural defects because of the weakness of the IR lines associated with the small concentrations of nitrogen that are present.

TABLE I. Concentrations of C and of O in mc-Si samples determined by FTIR measurements and the concentration of N in mc-Si samples determined by SIMS.

Sample	[C] (cm^{-3})	[O] (cm^{-3})	[N] (cm^{-3})
K(T)	8.2×10^{17}	1.0×10^{17}	2×10^{16}
K(B)	6.0×10^{17}	3.2×10^{17}	7×10^{15}
A(T)	4.6×10^{17}	1.2×10^{17}	4.7×10^{15}
A(B)	1.2×10^{17}	4.7×10^{17}	2.7×10^{15}
E(T)	2.3×10^{17}	0.4×10^{17}	7.9×10^{15}
E(B)	0.3×10^{17}	0.7×10^{17}	5.7×10^{15}

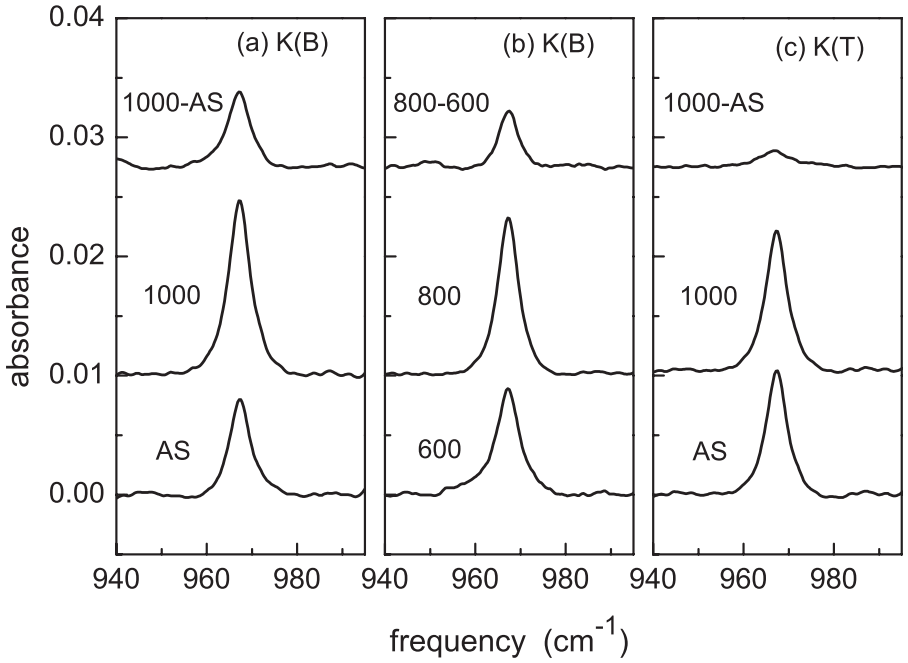

FIG. 2. Absorption spectra (77 K, resolution 1 cm^{-1}) of the 967 cm^{-1} line of the NN center in mc-Si. (a) Samples were prepared from test slab K(B) in the as-solidified state (bottom), annealed for 30 min at 1000 °C (center), and the difference of these spectra (top). (b) Samples were prepared from test slab K(B) and annealed for 15 h at 600 °C (bottom), annealed for 90 min at 800 °C (center), and the difference of these spectra (top). (c) Samples prepared from test slab K(T) in the as-solidified state (bottom), annealed for 30 min at 1000 °C (center), and the difference of these spectra (top).

From the data shown in Fig. 1(a), it was determined that the peak absorption coefficient of the NN line at 77 K (967 cm^{-1}) is a factor of 1.58 times greater than the peak absorption coefficient at room temperature (963 cm^{-1}). This result and the calibration of Itoh *et al.*[22] [Eq. (1)] lead to the following calibration of the NN line at 77 K:

$$[N] = 1.2 \times 10^{17}\,cm^{-2}\,\alpha_{967}. \quad (2)$$

From the noise in the baseline of the spectrum shown in Fig. 1(a), we estimate a detection limit for [N] in mc-Si of 0.2×10^{15} cm^{-3} at 77 K.

Measurements were made in the far-IR to detect the electronic transitions of electrically active NO_n centers. For these experiments, samples that were approximately 0.5 mm thick were prepared from a selection of the mc-Si test slabs available to us. The infrared light used to measure the far IR spectra of these samples was passed through a Si filter held at room temperature and placed before the sample in order to remove any above-band-gap light from the probing beam. These samples could be illuminated from the side by a supplementary visible light source (120 Watt tungsten-halogen lamp) that was focused onto the face of the Si sample to populate donor and acceptor states in partially compensated samples.[14,34]

Annealing treatments were performed in a conventional tube furnace in a flowing N_2 ambient to manipulate the concentrations of the different N-containing centers.

III. NN CENTERS AND THEIR INTERACTION WITH OXYGEN

The properties of NN and NNO_n centers in mc-Si can be investigated by way of their vibrational spectra. IR spectra (77 K) are shown in Fig. 2(a) for mc-Si samples prepared from the test slab K(B) with the O, N, and C content shown in Table I. The lower spectrum in the panel shows the 967 cm^{-1}line due to the NN center for a sample in its as-grown state. The middle spectrum shows the result for a sample from the same test slab annealed at 1000 °C (30 min). The upper spectrum shows the absorption for the 1000 °C-annealed sample using the spectrum for the as-grown sample for reference. The peak absorption coefficients for these lines and the corresponding concentrations of nitrogen present in the form of NN complexes are shown in Table II.

TABLE II. Absorption coefficients at 967 cm^{-1} (77 K) and nitrogen concentrations determined with Eq. (2) for mc-Si samples. Results are shown for samples that had been annealed at 1000 °C to dissociate NNO_n complexes and for samples in their as-solidified state. The difference of these results, reflecting the concentration of N in the form of NNO_n complexes in as-solidified samples, is shown in the right column. (The uncertainty in the nitrogen concentration is 0.2×10^{15} cm^{-3}. The uncertainty in Δ[N] is twice this value).

Sample	α(1000) (cm^{-1})	$[N]_{1000}$ (cm^{-3})	α(AS) (cm^{-1})	$[N]_{AS}$ (cm^{-3})	Δ[N] (cm^{-3})
K(T)	0.0536	6.3×10^{15}	0.0477	5.6×10^{15}	0.7×10^{15}
K(B)	0.0667	7.8×10^{15}	0.0377	4.4×10^{15}	3.4×10^{15}
A(T)	0.0240	2.8×10^{15}	0.0267	3.1×10^{15}	-0.3×10^{15}
A(B)	0.0177	2.1×10^{15}	0.0136	1.6×10^{15}	0.5×10^{15}
E(T)	0.0350	4.1×10^{15}	0.0333	3.9×10^{15}	0.2×10^{15}
E(B)	0.0411	4.8×10^{15}	0.0363	4.2×10^{15}	0.6×10^{15}

For a sample cut from test slab K(B) in its as-solidified state, the concentration of nitrogen present in the form of NN complexes is $4.4 \times 10^{15}\,cm^{-3}$. Annealing at 1000 °C dissociates oxygen-containing NNO_n complexes,[14,24] increasing the concentration of nitrogen present as NN centers to $7.8 \times 10^{15}\,cm^{-3}$. These results show that 56% of the nitrogen is present as NN centers in the test slab in its as-solidified state and that 44% is present as NNO_n complexes that formed as the ingot cooled to room temperature following growth.

Figure 2(b) shows spectra for additional samples prepared from the same test slab, K(B). The lower spectrum in the panel was measured for a sample annealed for 15 h at 600 °C. The middle spectrum is for a sample annealed at 800 °C (90 min) to dissociate NNO_n complexes. And the upper spectrum shows the difference of these results. The fraction of N present in the form of NNO_n centers is changed little by an extended anneal at 600 °C, showing that NN centers were complexed effectively with O as the mc-Si ingot was cooled to room temperature following solidification.

Figure 2(c) shows spectra for samples prepared from the test slab, K(T). The lower spectrum in the panel was measured for an as-solidified sample. The middle spectrum is for a sample annealed at 1000 °C (30 min). And the upper spectrum shows the difference of these results. The fraction of N present in the form of NN centers is increased to 89% for test slab K(T) cut from the top of the ingot, consistent with its lower concentration of interstitial oxygen ($1.0 \times 10^{17}\,cm^{-3}$ from Table I).

Table II contains a summary of our data for the concentrations of NN centers in as-solidified and annealed (1000 °C) samples for the six mc-Si test slabs that we studied. These data are also plotted in Fig. 3 along with the results for nitrogen in FZ Si and in Cz Si reported in the early study by Itoh *et al.*[22]

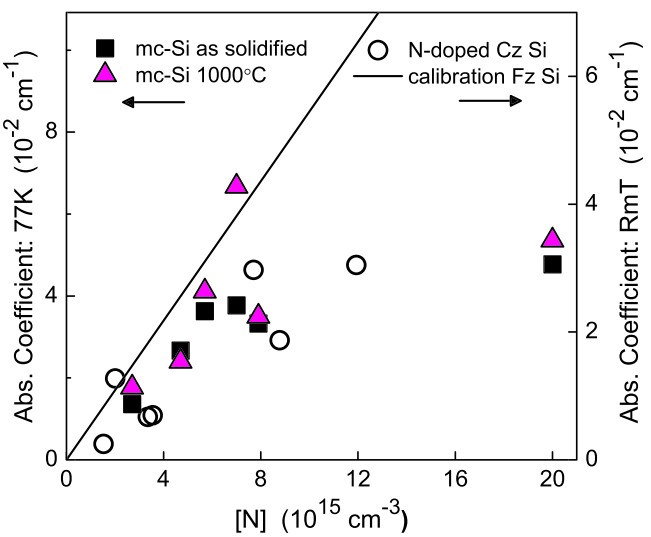

FIG. 3. Plot of absorption coefficient vs nitrogen concentration. The right (left) scale shows the absorption coefficient measured at room temperature (77 K). The solid line shows a calibration of the nitrogen concentration determined by Itoh *et al.*[22] from data for FZ Si. The open circles are data for Cz Si reported by Itoh *et al.*[22] The filled squares are data for mc-Si samples in their as-solidified state. The filled triangles are for mc-Si samples annealed at 1000 °C (30 min). The mc-Si test slab for these data, from left to right, are A(B), A(T), E(B), K(B), E(T), and K(T).

Itoh *et al.* plotted the absorption coefficient for the 963 cm^{-1} line (room temperature) assigned to the NN center vs. the concentration of nitrogen determined independently by neutron activation analysis.[22] We have constructed a similar plot (Fig. 3), including our IR data for mc-Si and the nitrogen concentrations for these samples determined by SIMS. For FZ Si containing little oxygen, Itoh *et al.* found that their plot of α_{963}(FZ) vs [N] yielded the straight line shown in Fig. 3 from which the calibration of the absorption coefficient of the 963 cm^{-1} line was determined (Eq. (1)).[22] These data are referenced to the right vertical axis showing the absorption coefficient of the 963 cm^{-1} line measured at room temperature. The open circles in Fig. 3 (right vertical axis) are the results of Itoh *et al.* for oxygen rich, Cz Si.[22] These data points lie below the calibration line because a portion of the nitrogen in oxygen-rich Si samples is in the form of NNO_n complexes.

The left vertical axis in Fig. 3 shows the peak absorption coefficient of the NN line at $967\,cm^{-1}$ measured at 77 K. The left axis has been scaled to correspond to the right axis, for the absorption coefficient measured at room temperature, that is, scaled by the factor 1.58 determined from the IR data shown in Fig. 1. The filled squares in Fig. 3 are data points, absorption coefficient at $967\,cm^{-1}$ (77 K) vs [N] measured by SIMS, for mc-Si samples in their as-solidified state, prepared from the six test slabs we investigated. These data lie below the calibration line determined for FZ Si, similar to the results of Itoh *et al.* for Cz Si.[22] These data show that not all nitrogen in mc-Si is present in the form of NN complexes, similar to the case of Cz Si, and as was also shown by the IR data presented in Fig. 2.

The filled triangles in Fig. 3 are for mc-Si samples annealed at 1000 °C. For 5 of our 6 test slabs, annealing at 1000 °C caused the concentration of the NN center to increase. And for the one sample where there appeared to be a small decrease in the concentration of NN centers, the size of this decrease is similar to the error in our IR measurements. For the four test slabs whose data points are shown closer to the left of Fig. 3, the filled triangles lie close to the calibration line determined by Itoh *et al.*[22] These results show that the nitrogen concentrations we have determined by SIMS are consistent with the neutron activation analysis results of Itoh *et al.*, and that following an anneal at 1000 °C, most of the nitrogen in mc-Si samples is in the form of NN centers. For the two samples whose data points are shown closer to the right of Fig. 3, the filled triangles lie well below the calibration line determined by Itoh *et al.* These results show that the distribution of nitrogen in mc-Si is more inhomogeneous than in monocrystalline Si, either FZ- or Cz-grown. Furthermore, SIMS is a local measurement and could be probing the properties of Si_3N_4 or Si-oxynitride precipitates which can be present in mc-Si,[17] giving what appears to be an anomalously large value for the nitrogen concentration ($2 \times 10^{16}\,cm^{-3}$) for one of our samples.

Trends can be seen in the data for mc-Si test slabs presented in Table II and Fig. 3. For each of the test slabs cut from the bottom of an ingot, there was a larger fraction of nitrogen present as NNO_n complexes when compared with a

test slab cut from the top of the same ingot. This result is consistent with the study of Kusunoki *et al.*[31] The test slabs with the highest oxygen content [K(B) and A(B)] had the largest fraction of N present as NNO_n centers (44% and 24%, respectively). And test slabs with the lowest oxygen content [A(T) and E(T)] showed almost no change in the intensity of the NN line at 967 cm^{-1} upon annealing at 1000 °C indicating that almost all nitrogen is present as NN centers without oxygen.

What oxygen-containing NNO_n complexes are present in our mc-Si test slabs? We use a strategy suggested by Alt and Wagner[14] to reduce the influence of multiphonon absorption on the spectrum of the weak vibrational lines due to nitrogen- and oxygen-containing complexes; a reference spectrum, recorded for a sample in its as-grown state, is subtracted from a spectrum of a sample from the same test slab annealed at 1000 °C. Fig. 4 shows such difference spectra for the mc-Si test slabs we have studied. The NNO_n and O_n complexes eliminated by an anneal at 1000 °C are shown as downward going features in the spectrum. NN centers without O whose intensities are increased by annealing at 1000 °C are shown as upward going features.

Alt and Wagner have tabulated the assignments of the IR features in this spectral region in Table II of Ref. 14. We have labeled the peaks in Fig. 4 according to these assignments. We note several trends in our spectral data

(i) Test slab K(B) has relatively high N and O concentrations for this set of mc-Si test slabs and contains the strongest IR features for the oxygen-containing NNO and NNO_2 complexes. A hint of the oxygen dimer, O_{2i}, is also seen in this spectrum. Test slab K(T) also has relatively high [N] but lower [O]. In this case, the IR lines associated with the NNO and NNO_2 centers are also seen but with reduced intensity.

(ii) Test slab A(B) has relatively high [O] but lower [N]. In this case, the NNO center is clearly seen and the oxygen dimer and trimer defects play a more important role. The oxygen concentration is reduced in test slab A(T), and the O_{2i} and O_{3i} complexes containing oxygen alone are no longer clearly seen.

(iii) Test slab E(B) contains O and N concentrations similar to those of sample K(T). The IR lines assigned to NNO complexes are seen for test slab E(B) with intensities similar to those of test slab K(T). Test slab E(T) has the lowest O content of the materials studied and shows only a barely detectable concentration of NNO centers.

(iv) A difference spectrum for a sample cut from test slab K(B), annealed for 16 h at 600 °C to produce oxygen containing centers is shown. Its partner in the difference spectrum was a sample from the same test slab annealed at 800 °C to dissociate NNO complexes. The difference spectrum is similar to that measured for an as-solidified sample. This result shows that the concentration of NNO_n centers formed while an ingot cools to room temperature is not increased substantially by further annealing at 600 °C.

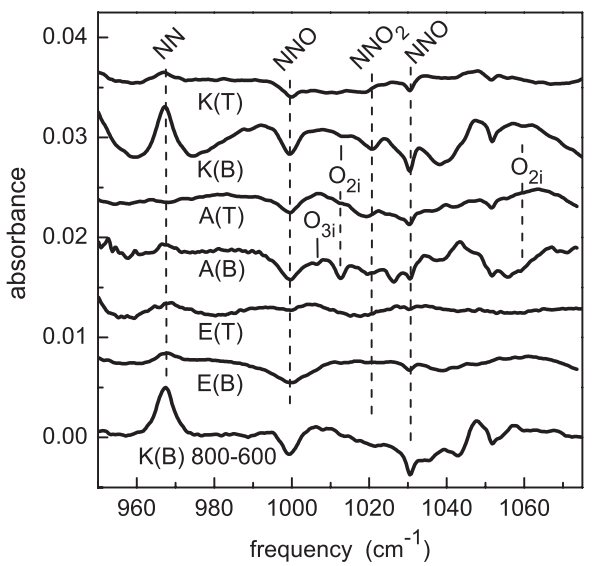

FIG. 4. The upper 6 spectra are differences between a mc-Si sample annealed at 1000 °C (30 min) and a sample from the same test slab in its as-solidified state. The bottom spectrum is a difference between a sample annealed at 800 °C (90 min) and a sample annealed for a long time at 600 °C (16 h) for test slab K(B).

IV. NO_n SHALLOW DONORS

Vibrational spectroscopy finds that mc-Si materials containing nitrogen and oxygen with concentrations in the neighborhood of 4×10^{15} cm^{-3} and 4×10^{17} cm^{-3}, respectively, can contain up to a few times 10^{15} cm^{-3} NNO_n complexes. These NNO_n complexes are electrically inactive. We turn now to NO_n complexes with a single N atom that acts as shallow thermal donors. While these defects do not show substantial vibrational absorption in our experiments, they may be detected with high sensitivity by way of their electronic absorption lines in the far IR.[13]

We begin our far IR experiments with a study of nitrogen-doped, p-type, Cz-grown Si with a nominal resistivity of 10–15 Ω cm, an oxygen concentration of $[O] = 7 \times 10^{17}$ cm^{-3}, and a carbon concentration of $[C] < 5 \times 10^{15}$ cm^{-3}. An IR measurement (77 K) of the 967 cm^{-1} line yielded a nitrogen concentration of $[N] = 1.8 \times 10^{15}$ cm^{-3}. These experiments on Cz Si provide a baseline for our study of mc-Si.

Cz Si samples with thicknesses 0.5 mm were prepared for our measurements in their as-grown state and by annealing at 600 °C for 15 h to produce NO_n shallow thermal donors.[14] Far IR absorption spectra for the boron acceptor and NO_n shallow donors are shown in Fig. 5(a) for the sample annealed at 600 °C. The lower spectrum in panel (a) shows the well-known boron-acceptor lines[35] labeled 1 and 2 at 245 and 278 cm^{-1}. This measurement was made with a probing beam that had been filtered to remove above band-gap light and without supplementary illumination. In this case, any lines that might arise from shallow donors are not seen. With supplementary illumination from the side with above band-gap light [upper spectrum in panel (a)], the intensities of the boron lines are observed to be increased because holes have been produced that fully populate the partially compensated shallow acceptor centers.[34] Furthermore, the upper spectrum in Fig. 5(a) shows the electronic transitions of shallow donors that have become populated by electrons produced by the side illumination. (We varied the intensity of the supplementary illumination

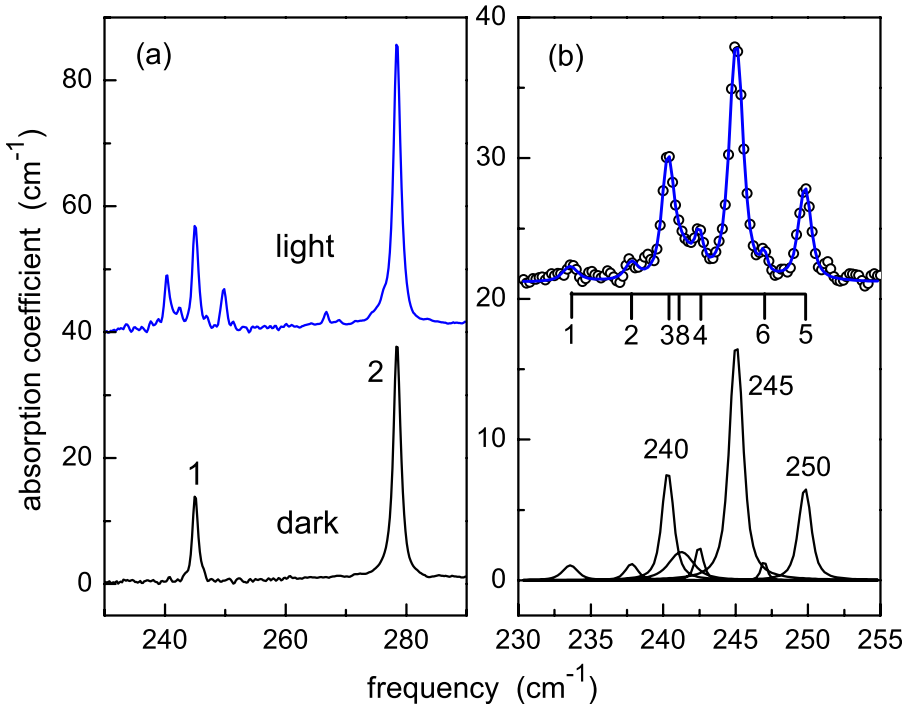

FIG. 5. Far IR absorption spectra (4.2 K, resolution 0.5 cm^{-1}) for Cz-grown Si annealed at 600 °C (15 h). (a) The lower spectrum was measured without supplementary illumination. Lines 1 and 2 of the boron acceptor at 245 and 278 cm^{-1} are shown. The upper spectrum was measured with supplementary illumination with above band-gap light, producing the absorption lines due to NO_n shallow donors. (b) Open circles in the upper spectrum show an expansion of the NO_n spectrum shown in (a). Assignments to the 1 s to $2p_{\pm}$ transitions of specific donor centers are shown. The thick solid line shows a fit to the measured spectrum with the sum of the Voigt line shape components shown below.

to insure that the intensities of the boron and NO_n lines had been saturated in these measurements.)

We use these results to calibrate the intensities of the NO_n shallow donors with optical measurements. A spectrum for the as-grown Cz-Si sample was measured to determine the concentration of boron. From the area of the 278 cm^{-1} line of the boron acceptor and the calibration,[36] $[B] = 1.5 \times 10^{13}$ cm^{-1} A_{278}, where A_{278} is the integrated area of the 278 cm^{-1} line, a boron concentration of 1.32×10^{15} cm^{-3} was obtained. A similar measurement was made in the absence of above band-gap illumination for the Cz Si sample that had been annealed at 600 °C (15 h) to determine the concentration of uncompensated boron. From the integrated area of the 278 cm^{-1} line, we obtained a value of 1.02×10^{15} cm^{-3}. These results show that the concentration of compensated boron and, therefore, of compensating NO_n donors produced by the 600 °C anneal is 0.30×10^{15} cm^{-3}.

Fig. 5(b) shows an expansion of the spectrum due to the 1 s to $2p_{\pm}$ transitions of the family of NO_n shallow donors along with the line at 245 cm^{-1} due to boron. The lines are labeled with their assignments given by Suezawa *et al.*[10] and by Alt *et al.*[30] We fit the 1s to $2p_{\pm}$ lines with a sum of Voigt line shapes as shown in the figure. The total area of the 1s to $2p_{\pm}$ transitions of the seven NO_n shallow donors that are seen was found to be 26.1 cm^{-2}. This result and our determination of the concentration of compensating centers in the sample lead to the calibration

$$[NO_n] = 1.1 \times 10^{13}\,\text{cm}^{-1}\,A_{NO}, \tag{3}$$

where A_{NO} is the integrated absorption coefficient for the 1s to $2p_{\pm}$ transitions of the family of NO_n shallow donors.[37] This calibration factor is very close to the calibrations found for the 1s to $2p_{\pm}$ transitions of the P, As, and Sb shallow donors in Si reported by Alt *et al.*[38] and by Porrini *et al.*[36]

Figure 6(a) shows IR spectra for the mc-Si sample A(B). The sample is p-type with a resistivity of approximately 1 Ω cm and had been annealed at 600 °C (15 h) to

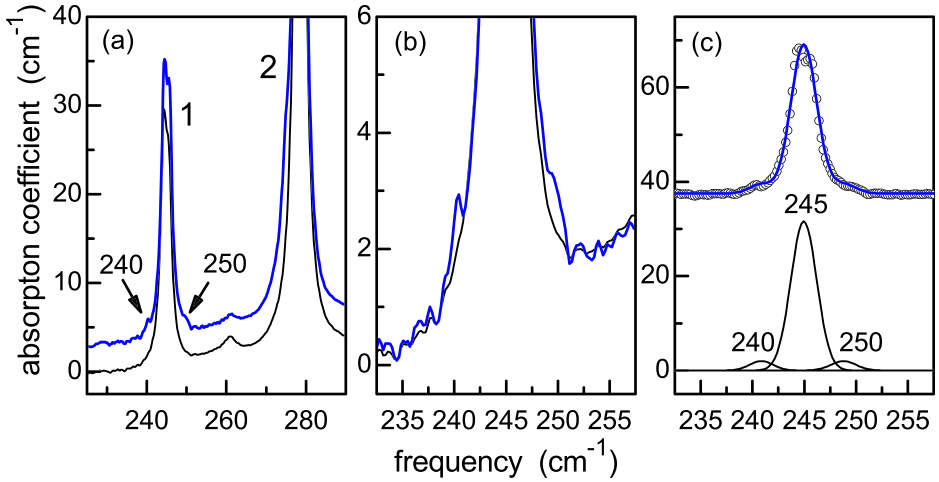

FIG. 6. Far IR absorption spectra (4.2 K, resolution 0.5 cm^{-1}) for a mc-Si sample prepared from test slab A(B) and annealed at 600 °C (15 h). (a) The lower spectrum was measured without supplementary illumination. The upper spectrum was measured with supplementary illumination with above band-gap light, to reveal the absorption lines at 240 and 250 cm^{-1} due to the NO-3 and NO-5 shallow donors, respectively. (b) An expansion of (a) showing the 240 and 250 cm^{-1} lines more clearly. (c) Open circles in the upper spectrum show an expansion of the region near 245 cm^{-1}. The solid line is a fit to the measured spectrum with the sum of the line shape components shown below.

increase the concentration of NO_n shallow thermal donors. The spectrum is dominated by the electronic transitions of the boron acceptor at 245 and 278 cm^{-1}. The lower spectrum in panel (a) shows no hint of the 1s to $2p_{\pm}$ lines of the NO_n shallow donors. However, the upper spectrum, measured in the presence of supplementary visible illumination, shows weak lines at the frequencies 240 and 250 cm^{-1} characteristic of the shallow thermal donors NO-3 and NO-5, respectively.[14,30] Figure 6(b) shows an expansion of the spectrum measured with above band-gap illumination where the lines at 240 and 250 cm^{-1} can be seen more clearly. Figure 6(c) shows a fit of the 245 cm^{-1} line due to boron and of the 240 and 250 cm^{-1} lines due to the NO-3 and NO-5 shallow donors. The open-circle curve symbols show the measured spectrum with the fit to these data passing through them. The individual line-shape components are shown below. The total area of the 240 and 250 cm^{-1} lines is 12 cm^{-2}, corresponding to a concentration of NO_n shallow donors of $[NO_n] = 1.3 \times 10^{14}$ cm^{-3} [determined with the calibration, Eq. (3)].[39]

We have characterized the concentration of NO_n centers in additional test slabs and with different heat treatments. Samples were prepared from the test slab K(B). A far-IR spectrum of a sample annealed at 600 °C (17 h) showed the weak lines at 240 and 250 cm^{-1} due to the shallow donors NO-3 and NO-5, similar to the case of test slab A(B) discussed above. From the total area of these lines, a concentration of shallow thermal donors of $[NO_n] = 8.5 \times 10^{13}$ cm^{-3} was determined.

A sample from test slab K(B) was annealed at 800 °C (90 min) to dissociate NO_n complexes. In this case, the lines at 240 and 250 cm^{-1} could not be detected in a far-IR spectrum measured with supplementary illumination. Furthermore, we prepared a sample from test slab E(T) that had the lowest oxygen content (0.4×10^{17} cm^{-3}) of the mc-Si test slabs available to us. In this case, we also could not detect any of the far-IR lines associated with NO_n shallow donors.

The magnitudes of the concentrations of NO_n shallow donors in our mc-Si samples can be estimated from the result found here for a Cz Si sample annealed at 600 °C and the dependence of the concentrations of NO_n donors on the concentrations of N and O found by Voronkov *et al.*[12] and by Wagner *et al.*[29] Voronkov *et al.*[12] found that the concentration of NO_n shallow donors is proportional to $[N]^{1/2}[O]^n$ with n between 2.75 and 3.25. Wagner *et al.*[29] found that NO-5 depends linearly on [O] whereas NO-3 is proportional to $[O]^2$. The result that the shallow donors NO-5 and NO-3 are dominant in our mc-Si samples, suggests an approximate dependence of the NO_n donor concentration on the nitrogen and oxygen concentrations of $[NO_n] \propto [N]^{1/2}[O]^2$.

Our Cz-grown Si sample with $[N] = 1.8 \times 10^{15}$ cm^{-3} and $[O] = 7 \times 10^{17}$ cm^{-3} showed an NO_n donor concentration of 3×10^{14} cm^{-3} following a long anneal at 600 °C. The mc-Si test slab A(B) has $[N] = 2.8 \times 10^{15}\,cm^{-3}$ and $[O] = 4.7 \times 10^{17}\,cm^{-3}$, suggesting that the NO_n concentration will be reduced by a factor of $(2.8/1.8)^{1/2}(4.7/7)^2 = 0.56$ compared with the result for our Cz Si sample to yield an estimated concentration of $[NO_n] = 1.7 \times 10^{14}\,cm^{-3}$. Similarly, mc-Si test slab K(B) has $[N] = 7.8 \times 10^{15}\,cm^{-3}$ and $[O] = 3.2 \times 10^{17}\,cm^{-3}$, yielding an estimated concentration of NO_n donors of $1.3 \times 10^{14}\,cm^{-3}$. These estimated values of the NO_n donor concentrations in mc-Si samples are only small factors greater than the values measured by our far-IR spectra. When the oxygen concentration is reduced substantially, as for the case of test slab E(T) with $[O] = 0.4 \times 10^{17}\,cm^{-3}$, the NO_n concentration should be reduced to well below the detection limit for NO_n donors in our experiments, in agreement with our observations here. The success of these simple estimates shows that the magnitude of the NO_n concentration in mc-Si is in reasonable agreement with the dependences on the concentrations of N and O found previously for monocrystalline Si.[12,29]

V. CONCLUSION

We have studied the properties of nitrogen- and oxygen-containing point defects in mc-Si used for the fabrication of solar cells. The N- and O-containing point defects in a set of mc-Si test slabs with [N] varying from 2.1 to 7.8×10^{15} cm^{-3} (Table II) and [O] varying from 0.4 to 4.7×10^{17} cm^{-3} (Table I) have been investigated by low-temperature IR spectroscopy to identify the defects that are present and to determine their concentrations.

The vibrational spectroscopy of the LVM's of nitrogen-containing complexes showed that nitrogen in our mc-Si samples is present predominantly in the form of NN and NNO_n complexes, with the fraction present as NNO_n centers being sensitive to the oxygen content of the sample. The concentration of NNO_n complexes was found to be as high as 3.4×10^{15} cm^{-3}, accounting for 44% of the sample's N content, for a mc-Si test slab with an oxygen concentration of $[O] = 3.2 \times 10^{17}$ cm^{-3}. Other test slabs had an oxygen concentration as low as $[O] = 0.4 \times 10^{17}$ cm^{-3}, and in this case, NNO_n centers were barely detectable. NNO_n complexes were present in our mc-Si test slabs in their as-solidified state, and their concentration was not changed significantly by long anneals at 600 °C. Presumably NNO_n centers were formed as a mc-Si ingot was cooled to room temperature following its solidification.

The carbon concentration in our mc-Si test slabs also varied over a wide range, from 0.3 to 8.2×10^{17} cm^{-3}. We did not detect changes in the nitrogen-containing defects formed in our experiments that could be attributed to carbon.

Our mc-Si materials also contained electrically active NO_n shallow donors that could be detected with high sensitivity by their electronic transitions in the far IR.[10,11,13] A concentration of NO_n shallow donors as high as 1.3×10^{14} cm^{-3} was found in a mc-Si sample with $[O] = 4.7 \times 10^{17}$ cm^{-3}. The concentration of NO_n shallow donors is approximately 100 times smaller than the concentration of boron acceptors and has little effect on the compensation of the p-type mc-Si substrate.

In a test slab with a low oxygen concentration ($[O] = 0.4 \times 10^{17}\,cm^{-3}$), NO_n shallow donors were not detected by our measurements.

The properties of nitrogen- and oxygen-containing point defects in mc-Si can be explained well from what has been learned in previous studies of nitrogen-containing defects in

monocrystalline Si. What distinguishes mc-Si from Cz Si is the large range over which the concentrations of nitrogen and oxygen can vary in mc-Si. And the defects that form are sensitive to this variation in the impurity content of the mc-Si substrate.

ACKNOWLEDGMENTS

The work performed at Lehigh University has been supported by the Silicon Solar Research Center SiSoC Members through NCSU Subaward No. 2008-0519-02, NSF Grant No. 1160756, and a Faculty Incentive Research Grant from Lehigh University.

[1]M. Suezawa, in *Properties of Crystalline Silicon*, edited by R. Hull (INSPEC, London, 1999), p. 538.
[2]K. Sumino, I. Yonenaga, M. Imai, and T. Abe, J. Appl. Phys. **54**, 5016 (1983).
[3]I. Yonenaga, J. Appl. Phys. **98**, 023517 (2005).
[4]C. R. Alpass, J. D. Murphy, R. J. Falster, and P. R. Wilshaw, J. Appl. Phys. **105**, 013519 (2009).
[5]T. Abe and K. Kimura, *in Semiconductor Silicon 1990*, edited by H. R. Huff, K. Barraclough, and J. Chikawa (Electrochemical Society, Pennington, NJ, 1990), p. 105.
[6]W. V. Ammon, P. Dreier, W. Hensel, U. Lambert, and L. Köster, Mater. Sci. Eng. B **36**, 33 (1996).
[7]D. Gräf, M. Suhren, U. Lambert, R. Schmolke, A. Ehlert, W. Von Ammon, and P. Wagner, J. Electrochem. Soc. **145**, 275 (1998).
[8]M. Iida, W. Kusaki, M. Tamatsuka, E. Iino, M. Kimura, and S. Muraoka, *in Defects in Silicon III*, edited by T. Abe, W. M. Bullis, S. Kobayashi, W. Lin, and P. Wagner (Electrochemical Society, Pennington, NJ, 1999), p. 499.
[9]V. V. Voronkov and R. Falster, J. Cryst. Growth **273**, 412 (2005).
[10]M. Suezawa, K. Sumino, H. Harada, and T. Abe, Jpn. J. Appl. Phys. Part 2 **25**, L859 (1986).
[11]H. Navarro, J. Griffin, J. Weber, and L. Genzel, Solid State Commun. **58**, 151 (1986).
[12]V. V. Voronkov, M. Porrini, P. Collareta, M. G. Pretto, R. Scala, R. Falster, G. I. Voronkova, A. V. Batunina, V. N. Golovina, L. V. Arapkina, A. S. Guliaeva, and M. G. Milvidski, J. Appl. Phys. **89**, 4289 (2001).
[13]H. Ch. Alt, Y. V. Gomeniuk, F. Bittersberger, A. Kempf, and D. Zemke, Appl. Phys. Lett. **87**, 151909 (2005).
[14]H. Ch. Alt and H. E. Wagner, J. Appl. Phys. **106**, 103511 (2009).
[15]B. Wu, N. Stoddard, R. Ma, and R. Clark, J. Cryst. Growth **310**, 2178 (2008).
[16]H. Rodriguez, I. Guerrero, W. Koch, A. L. Endrös, D. Franke, C. Häβler, J. P. Kalejs, and H. J. Möller, *in Handbook of Photovoltaic Science and Engineering*, 2nd ed., edited by A. Luque and S. Hegedus (Wiley, 2011), p. 218.
[17]H. J. Möller, T. Kaden, S. Scholz, and S. Würzner, Appl. Phys. A **96**, 207 (2009).
[18]H. J. Stein, Appl. Phys. Lett. **43**, 296 (1983).
[19]H. J. Stein, *Proceedings of the 13th International Conference on Defects in Semiconductors*, edited by L. C. Kimerling and J. M. Parsey, Jr. (Metallurgical Society of AIME, Warrendale, PA, 1985), p. 839.
[20]R. Jones, S. Öberg, F. Berg Rasmussen, and B. Bech Nielsen, Phys. Rev. Lett. **72**, 1882 (1994).
[21]J. P. Goss, I. Hahn, R. Jones, P. R. Briddon, and S. Öberg, Phys. Rev. B **67**, 045206 (2003).
[22]Y. Itoh, T. Nozaki, T. Masui, and T. Abe, Appl. Phys. Lett. **47**, 488 (1985).
[23]P. Wagner, R. Oeder, and W. Zulehner, Appl. Phys. A **46**, 73 (1988).
[24]M. W. Qi, S. S. Tan, B. Zhu, P. X. Cai, W. F. Gu, X. M. Xu, T. S. Shi, D. L. Que, and L. B. Li, J. Appl. Phys. **69**, 3775 (1991).
[25]A. Gali, J. Miro, P. Deák, C. P. Ewels, and R. Jones, J. Phys. Condens. Matter **8**, 7711 (1996).
[26]F. Berg Rasmussen, S. Öberg, R. Jones, C. Ewels, J. Goss, J. Miro, and P. Deák, Mater. Sci. Eng. B **36**, 91 (1996).
[27]F. Sahtout Karoui and A. Karoui, J. Appl. Phys. **108**, 033513 (2010).
[28]N. Fujita, R. Jones, S. Öberg, and P. R. Briddon, Appl. Phys. Lett. **91**, 051914 (2007).
[29]H. E. Wagner, H. Ch. Alt, W. von Ammon, F. Bittersberger, A. Huber, and L. Koester, Appl. Phys. Lett. **91**, 152102 (2007).
[30]H. Ch. Alt, H. E. Wagner, W. von Ammon, F. Bittersberger, A. Huber, and L. Koester, Physica B **401–402**, 130 (2007).
[31]H. Kusunoki, T. Ishizuka, A. Ogura, and H. Ono, Appl. Phys. Express **4**, 115601 (2011).
[32]G. Davies and R. C. Newman, *in Handbook on Semiconductors, Materials, Properties, and Preparation*, edited by S. Mahajan and T. S. Moss (North-Holland, Amsterdam, 1994), Vol. 3B, p. 1557.
[33]A. Baghdadi, W. M. Bullis, M. C. Croarkin, Y.-Z. Li, R. I. Scace, R. W. Series, P. Stallhofer, and M. Watanabe, J. Electrochem. Soc. **136**, 2015 (1989).
[34]B. O. Kolbesen, Appl. Phys. Lett. **27**, 353 (1975).
[35]B. Pajot, *Optical Absorption of Impurities and Defects in Semiconducting Crystals* (Springer, Heidelberg, 2010), pp. 282–293.
[36]M. Porrini, M. G. Pretto, R. Scala, A. V. Batunina, H. Ch. Alt, and R. Wolf, Appl. Phys. A **81**, 1187 (2005).
[37]A calibration of the peak heights of the NO_n lines (rather than of the line areas) based on Hall effect measurements was reported previously by Voronkov *et al*.[12] If we apply this calibration to the sum of the peak heights determined from our fit to the 1s to $2p_{\pm}$ transitions of the family of NO_n shallow donors shown in Fig. 5(b), we calculate a concentration of NO_n donors that is three times larger than the result we have determined here from the compensation condition of the sample. Therefore, even though a direct comparison is difficult because we have calibrated the line areas of the 1s to $2p_{\pm}$ transitions of the NO_n centers and Voronkov *et al*. have calibrated the peak heights, our calibration factor is approximately a factor of 3 times smaller than is suggested by the calibration reported previously by Voronkov *et al*.
[38]H. Ch. Alt, M. Gellon, M. G. Pretto, R. Scala, F. Bittersberger, K. Hesse, and A. Kempf, *in CP449, Characterization and Metrology for ULSI Technology: 1998 International Conference*, edited by D. G. Seiler, A. C. Diebold, W. M. Bullis, T. J. Shaffner, R. McDonald, and E. J. Walters (American Institute of Physics, New York, 1998), p. 201.
[39]To estimate the error in our measurement of the areas of the weak lines at 240 and 250 cm^{-1}, we have made an independent IR measurement and fit of the IR lines at 240, 245, and 250 cm^{-1} shown in Fig. 6(c). The total area of the weak lines at 240 and 250 cm^{-1} varied by 25% between measurements. A discrepancy as large as 50% would not have been surprising, given the overlap of the weak lines at 240 and 250 cm^{-1} with the much stronger line at 245 cm^{-1}. The uncertainties in calibrations such as Eq. (3) in the literature have sometimes been as large as a factor of 2. Therefore, the uncertainty in the calibration given in Eq. (3) is the primary source of uncertainty in our measurement of the absolute concentration of NO_n shallow donors, which we estimate to be near a factor of 2.